

## Spatial Fluctuations of Loose Spin Coupling in CuMn/Co Multilayers

T. Saerbeck,<sup>1,2,\*</sup> N. Loh,<sup>1,2</sup> D. Lott,<sup>3</sup> B. P. Toperverg,<sup>4,5</sup> A. M. Mulders,<sup>6,7,2</sup> A. Fraile Rodríguez,<sup>8,9</sup> J. W. Freeland,<sup>10</sup>  
M. Ali,<sup>11</sup> B. J. Hickey,<sup>11</sup> A. P. J. Stampfl,<sup>2,12</sup> F. Klose,<sup>2</sup> and R. L. Stamps<sup>1,13</sup>

<sup>1</sup>*School of Physics, University of Western Australia, Crawley, WA6009, Australia*

<sup>2</sup>*Australian Nuclear Science and Technology Organisation, Menai, NSW 2234, Australia*

<sup>3</sup>*Institute for Materials Research, Helmholtz Zentrum Geesthacht, 21502 Geesthacht, Germany*

<sup>4</sup>*Department of Physics, Ruhr-University Bochum, 44780 Bochum, Germany*

<sup>5</sup>*Petersburg Nuclear Physics Institute, 188350 Gatchina, Russia*

<sup>6</sup>*School of Physical, Environmental and Mathematical Sciences, UNSW in Canberra, ACT 2600, Australia*

<sup>7</sup>*Department of Imaging and Applied Physics, Curtin University of Technology, Perth, WA 6845, Australia*

<sup>8</sup>*Dept. Física Fonamental and Institut de Nanociència i Nanotecnologia (IN2UB),  
Universitat de Barcelona, 08028 Barcelona, Spain*

<sup>9</sup>*Swiss Light Source, Paul Scherrer Institut, CH-5232 Villigen, Switzerland*

<sup>10</sup>*Advanced Photon Source, Argonne National Laboratory, Argonne, Illinois 604389, USA*

<sup>11</sup>*School of Physics and Astronomy, University of Leeds, Leeds LS29JT, United Kingdom*

<sup>12</sup>*School of Chemistry, The University of Sydney, NSW 2006, Australia*

<sup>13</sup>*SUPA, School of Physics and Astronomy, University of Glasgow, Glasgow G12 8QQ, Scotland, United Kingdom*

(Received 14 March 2011; published 12 September 2011)

A detailed investigation of magnetic impurity-mediated interlayer exchange coupling observed in  $\text{Cu}_{0.94}\text{Mn}_{0.06}/\text{Co}$  multilayers using polarized neutron reflectometry and magnetic x-ray techniques is reported. Excellent descriptions of temperature and magnetic field dependent biquadratic coupling are obtained using a variant of the loose spin model that takes into account the distribution of the impurity Mn ions in three dimensions. Positional disorder of the magnetic impurities is shown to enhance biquadratic coupling via a new contribution  $J_2^{\text{fluct}}$ , leading to a temperature dependent canting of magnetic domains in the multilayer. These results provide measurable effects on RKKY coupling associated with the distribution of impurities within planes parallel to the interfaces.

DOI: 10.1103/PhysRevLett.107.127201

PACS numbers: 75.70.Cn, 75.30.Et, 75.30.Hx

Magnetic exchange coupling in the form of Ruderman-Kittel-Kasuya-Kittel (RKKY) interactions in magnetic thin films or multilayers is a fascinating and important phenomenon that has found great utility in magneto- and spin electronics [1]. Novel systems, incorporating dilute magnetic impurities in metallic multilayers [2], semiconductors [3], oxides [4], or insulators [5], exhibit a range of interesting phenomena based on exchange coupling through dilute impurity centers, the understanding of which is crucial for any future search for applicability or the tuning of physical properties [6].

Early observations of an orthogonal magnetic coupling in metallic multilayers [7] have been described with a loose spin coupling (LSC) model proposed by Slonczewski [8], describing the impurities as paramagnetic (PM) moments that interact with the magnetic layers. While LSC was able to account for the temperature dependence of biquadratic (BQ) coupling, unphysically large values for the exchange fields were required to account for the observed coupling strength [2,7,8]. We show that properly accounting for the spatial distribution of the impurities throughout the multilayer removes this limitation. Further, we find that the first order, bilinear LSC terms do not cancel out when averaged over different spin locations, as suggested previously [2,8]. Instead, we demonstrate how the random distribution of

spins leads to a lateral fluctuation which contributes to the net BQ coupling. Our results are therefore of consequence for the problem of RKKY coupling in general, especially since several encounters of magnetic impurity-mediated coupling in novel materials are examined in view of LSC [9,10]. By accounting for the natural random distribution, experimental observations of temperature dependent coupling angles and saturation fields in strongly BQ coupled  $\text{Cu}_{0.94}\text{Mn}_{0.06}/\text{Co}$  multilayers are reproduced using a single set of underlying RKKY exchange parameters.

We will focus on a sample structure  $\text{Ta}(50\text{Å})/[\text{Cu}_{0.94}\text{Mn}_{0.06}(19\text{Å})/\text{Co}(21\text{Å})]\times 30/\text{Ta}(25\text{Å})$ , where temperature dependent effects have been observed through magnetotransport studies [11]. The  $\text{Cu}_{0.94}\text{Mn}_{0.06}/\text{Co}$  multilayers were grown on Si(100) substrates at ambient temperatures by dc magnetron sputtering in  $3.3 \times 10^{-3}$  mbar Ar pressure, in a system with a base pressure of  $1 \times 10^{-8}$  mbar.

The magnetic structures of the ferromagnetic (FM) Co layers have been resolved using polarized neutron reflectometry (PNR) as a function of external field and temperature using NERO at the Helmholtz Zentrum Geesthacht (HZG), Germany. Full polarization analysis recording non-spin-flip (NSF),  $R^{++}$  and  $R^{--}$ , and spin-flip (SF),  $R^{+-}$  and  $R^{-+}$ , reflectivities is used to determine the

magnitude and direction of the magnetization vector in successive layers [12]. In such measurements  $R^{++}$  and  $R^{--}$  probe the projection  $M_{\parallel}$  of the magnetization vector onto the polarization direction (within the surface plane of the sample), while  $R^{+-}$  and  $R^{-+}$  are due to the component  $M_{\perp}$  normal to this direction. Figure 1(a) shows reflectivities along the momentum transfer  $Q_Z$ , normal to the surface, at 300 and 30 K as well as the corresponding simulations. The refined structural parameters, such as mass densities, individual thicknesses, and interface roughness, agree well with values determined by x-ray reflectometry and high angle neutron and x-ray diffraction, which confirm coherent growth along the Cu(111) direction. The first order Bragg peak at  $Q_Z = 0.158 \text{ \AA}^{-1}$ , observed at 300 K, corresponds to a bilayer periodicity of 40 Å. The difference between  $R^{++}$  and  $R^{--}$  indicates FM alignment of subsequent Co layers with an averaged magnetization of  $1.46 \pm 0.05 \mu_B/\text{atom}$  (bulk:  $1.53 \mu_B/\text{atom}$ ). Upon cooling of the system below 100 K, a magnetic half-order peak is

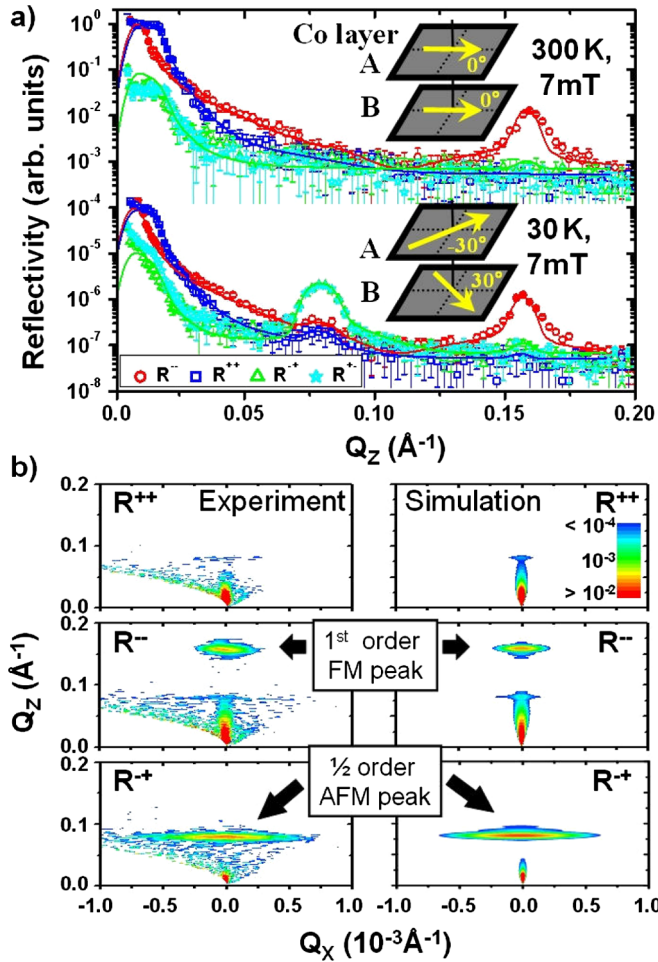


FIG. 1 (color online). (a) NSF (red circles, blue squares) and SF (green triangles, cyan stars) PNR data fitted to the model sketched in the inset. (b) Off-specular scattering at 30 K and 7 mT data (left) and simulations (right).

observed in  $R^{+-}$  and  $R^{-+}$  at  $Q_Z = 0.076 \text{ \AA}^{-1}$ , suggesting a canted magnetic structure with finite  $M_{\perp}$  and a doubling in periodicity due to alternating alignment of subsequent magnetizations.

While specular PNR as a function of  $Q_Z$  resolves depth profiles of nuclear and magnetic structures, the lateral wave vector transfer  $Q_X$  probes magnetic domains in the sample plane, via off-specular scattering [12]. As shown in Fig. 1(b), the SF signal is an intense off-specular scattering associated with the presence of lateral magnetic domains. Simulations of both the specular and off-specular data have been performed using a distorted wave Born approximation [Fig. 1(b), right] [12,13]. The increase in experimental background signal towards  $Q_Z = 0$  is not regarded in the simulations. The off-specular scattering related to the half-order peak at 30 K is well described by magnetic domains with a lateral size of  $0.43 \mu\text{m}$  and magnetizations alternatively canted in neighboring Co layers throughout the multilayer [Fig. 1(a), inset]. We find a canting of  $\phi_{1,2} = \pm 30^\circ$  with respect to the external guide field. Temperature and field dependence of the coupling angle  $\phi = \phi_1 - \phi_2$  are shown in Fig. 2(a). A more detailed description of the specular and off-specular analysis will be presented elsewhere [14].

From the temperature and field dependence of the Co coupling angle  $\phi$ , the interlayer exchange energies  $J_1$  and  $J_2$  are determined over the magnetic areal density  $E(\phi)$  [2]. Assuming negligible in-plane anisotropy,

$$E(\phi) = -MdH \cos\left(\frac{\phi}{2}\right) - J_1 \cos(\phi) + J_2 \cos^2(\phi), \quad (1)$$

where  $H$  is the external field,  $M$  the volume magnetization, and  $d$  the thickness of the FM layers.  $J_1$  and  $J_2$  are deduced by energy minimization of Eq. (1) [15] and found to increase below a temperature where the canted magnetization appears [Fig. 2(b); theoretical fits are discussed later].

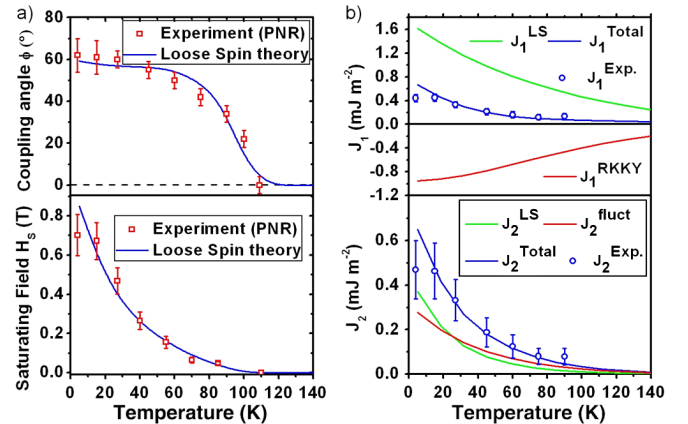


FIG. 2 (color online). (a) Coupling angle and saturation field as determined by PNR (symbols) and theoretical fits (lines). (b) Experimental coupling terms (symbols) and model exchange coupling components (lines).

In order to identify correlations between the BQ coupling and the magnetic state of the dilute magnetic impurities, we now turn to an element specific investigation using polarized x-ray absorption spectroscopy (XAS). Figure 3 shows XAS at the Mn  $L_{2,3}$  edges for left ( $\sigma^-$ ) and right ( $\sigma^+$ ) circular polarization of the biquadratically coupled state ( $T = 70$  K,  $H = 50$  mT) [16]. Several multiplet features, as well as a large branching ratio  $I(L_3)/[I(L_3) + I(L_2)] = 0.75$ , are characteristic for a high spin state [17]. The qualitative shape of the multiplet features has been simulated with CTM4XAS [18] using a predominantly  $3d^5$  electron configuration with  $M_{\text{Mn}} = (4.4 \pm 0.4)\mu_B$ . The finite x-ray magnetic circular dichroism (XMCD), i.e., the difference between the  $\sigma^+$  and  $\sigma^-$  absorption cross section, indicates an increase in the net Mn magnetization towards lower temperature (Fig. 3). Both the Co and Mn XMCD have the same sign, demonstrating that the net Mn moment is orientated collinear to the Co magnetization, consistent with PM Mn spins polarized due to exchange interactions with the nearby FM layers. The observed similarity of element specific hysteresis loops of Co and Mn, recorded by x-ray resonant magnetic scattering (XRMS) in reflectivity at the  $L_3$  edges at the Advanced Photon Source, further supports this [19].

A model of the magnetic interaction between the FM Co layers must include the PM Mn spins as well as the Cu conduction electrons, defining the energies  $J_1 = J_1^{\text{RKKY}} + J_1^{\text{LSC}}$  and  $J_2 = J_2^{\text{LSC}} + J_2^{\text{fluct}}$ . Here  $J_1^{\text{RKKY}}$  is the RKKY exchange between FM Co layers [20],  $J_1^{\text{LSC}}$  and  $J_2^{\text{LSC}}$  are the loose spin couplings via the Mn spins [8]. In order to fully describe the coupling situation, we introduce a new contribution to the overall interlayer exchange coupling  $J_2^{\text{fluct}}$ , arising from random lateral distributions of the Mn impurities. Beyond the model of LSC, we will discuss lateral variations in  $J_1^{\text{LSC}}$ , derived by convolution with a random Mn distribution, which will lead to additional BQ coupling via fluctuation mechanisms [21]. A schematic of

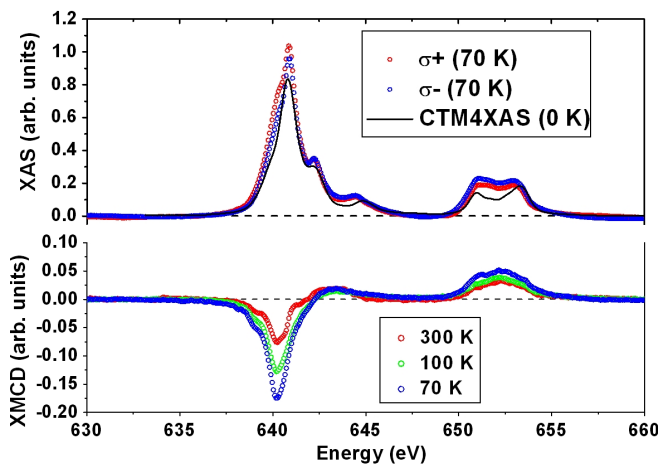


FIG. 3 (color online). Mn  $L_{2,3}$ -edge absorption and x-ray magnetic circular dichroism as a function of temperature.

the interlayer coupling situation is shown in Fig. 4(a). To include the lateral disorder in calculating  $J_1^{\text{LSC}}$ , one needs to consider the three-dimensional form of the RKKY interaction  $J^{\text{RKKY}} = C[2kr \cos(2kr + \Phi) - \sin(2kr + \Phi)] / (2kr)^4$  [20] between individual Co and Mn spins.  $k$  represents the frequency and  $\Phi$  the phase of the oscillation. For a single Mn spin, this interaction varies in the plane of the ferromagnets as a function of the distance  $s(x, y)$  [Fig. 4(a)]. The RKKY exchange fields  $\vec{U}_j$  of the ferromagnets are defined by  $J^{\text{RKKY}}$ , integrated over the plane of the ferromagnets,  $\vec{U}_A(z) = \vec{U}_B(t - z)$ , and are plotted in Fig. 4(c),

$$\vec{U}_j = \vec{B}_{\text{eff}} \frac{d_{\text{Cu}}^2}{z^2} \sin(q_z z + \Phi) \frac{zT/T_0 + T/T_0^i}{\sinh(zT/T_0 + T/T_0^i)}, \quad (2)$$

with amplitude  $|\vec{B}_{\text{eff}}|$ , oriented parallel to the corresponding ferromagnet, extremal spanning vector  $q_z$  for a lattice spacing  $d_{\text{Cu}}$  and characteristic temperatures  $T_0$  and  $T_0^i$  [22]. Since the orientation of the PM Mn spins is isotropic, the vector sum  $U(z) = |\vec{U}_A(z) + \vec{U}_B(z)|$  can be used to calculate the total exchange energies  $J_1^{\text{LSC}}$  and  $J_2^{\text{LSC}}$  according to the model from Slonczewski [8]:  $J_1^{\text{LSC}} = 1/2 \sum_{z_i} [F(z_i, \pi) - F(z_i, 0)]$  and  $J_2^{\text{LSC}} = \sum_{z_i} 1/2 [F(z_i, \pi) + F(z_i, 0)] - F(z_i, \pi/2)$ , where  $F[U(z, \phi)]$  is the free energy of the system. In order to account for the 3D structure of the exchange coupling, a summation over all impurity locations  $z_i$  in the Cu layer for collinear ( $\phi = \pi, 0$ ) and orthogonal alignment ( $\phi = \pi/2$ ) has been performed.

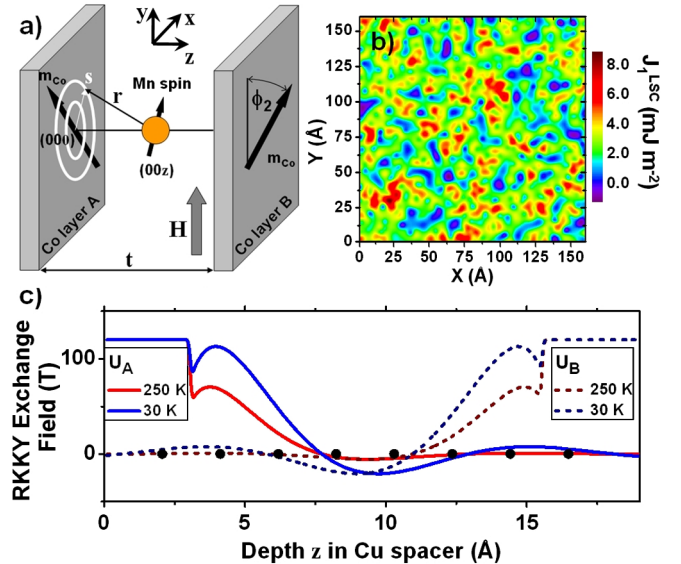


FIG. 4 (color online). (a) Schematic coupling of a PM Mn spin between two FM layers. (b) Calculated lateral variation of  $J_1^{\text{LSC}}$  at 30 K. (c) RKKY exchange fields acting on loose Mn atoms derived by fits to the experimental data. Black dots indicate (111) planes in the fcc lattice. The extended plateau on either side of the plot indicates Mn impurities in the direct vicinity of the Co layers experiencing direct magnetic exchange.

Going beyond the LSC model, we now consider the exchange interaction  $J_1^{\text{LSC}}$  calculated for collinear and orthogonal alignment of the interaction through a *single* Mn spin,  $J_{\text{Co-Mn}}^{\text{RKKY}}(x, y, z)$  and the right-hand ferromagnet  $U_B(z)$  [23]. A comprehensive 2D form of  $J_1^{\text{LSC}}(x, y)$  is obtained by a convolution with a random 6 at. % site occupancy of spins in the lateral dimension of the spacer, in which each Mn position is represented via a  $\delta$  function. Figure 4(b) shows the result of the lateral convolution, summed over  $z$  positions corresponding to the (111) lattice planes of the Cu spacer. In order to derive the new BQ coupling contribution,  $J_1^{\text{LSC}}(x, y)$  is decomposed into 2D Fourier components  $J_F(x, y) = a \sin(\pi x/l) \sin(\pi y/l)$ , where amplitude  $a$  and length scale  $l$  are chosen to resemble the length and energy fluctuations in  $J_1^{\text{LSC}}(x, y)$  [Fig. 4(b)]. The resulting expression for the additional BQ coupling [19,21] is

$$J_2^{\text{fluct}} = \frac{1}{4\sqrt{2}\pi A} \sum_i a_i l_i \coth\left(\frac{\sqrt{2}\pi d}{l_i}\right), \quad (3)$$

where  $A = 1.2 \times 10^{-8} \text{ Jm}^{-1}$  is the exchange stiffness of the Co layers.

The magnetic interaction energies  $J_1^{\text{RKKY}}$ ,  $J_1^{\text{LSC}}$ ,  $J_2^{\text{LSC}}$ , and  $J_2^{\text{fluct}}$  [Fig. 2(b)] are solely determined by the RKKY exchange parameters  $J^{\text{RKKY}}$  [Eq. (2)] and the Mn moment. The phase and period of the RKKY are estimated from results on Co/Cu(111) multilayers [24]. A substantial  $J_1^{\text{LSC}}$  contribution exists even after the summation over Mn positions, but the opposite sign of  $J_1^{\text{RKKY}}$  and  $J_1^{\text{LSC}}$  and the new contribution from  $J_2^{\text{fluct}}$  describe our experimental findings very well. The best fit gives  $B_{\text{eff}} = 540 \text{ T}$ ,  $T_0 = 1000 \text{ K}$ ,  $T_0^i = 300 \text{ K}$ , and  $J_{\text{Co}}/J_{\text{Mn}} = 0.62$ , where  $J_{\text{Co}}/J_{\text{Mn}}$  describes an energy scaling to account for different hybridization between Cu conduction electrons and Co and Mn  $d$  electrons. These values are consistent with previous experimental works on Co/Cu(111) systems [22,24]. The Mn spins at the center of the Cu layer are aligned opposite to the Co moments [Fig. 4(c)] while the net Mn polarization is parallel to the Co moments in agreement with the XMCD and XRMS results. Investigations on a range of CuMn thicknesses all gave similar results, therefore indicating a phenomenon of greater generality rather than a special case of well-matched coupling terms [25].

In conclusion, we have shown how random positional disorder of dilute magnetic impurity atoms enhances biquadratic coupling by creating lateral variations in exchange. Our results highlight the influence of dilute magnetic impurities on the host system, which is of consequence for the problem of RKKY coupling in general. We demonstrate that, by taking into account all three dimensions of the interaction and positional disorder, a consistent model of conduction spin mediated interlayer coupling is obtained. Next to tailoring of artificial magnetic properties in metallic multilayers, the applicability of our

model to the general problem of impurity-mediated exchange coupling will improve the understanding of biquadratic coupling in Heusler alloys [26] and dilute magnetic semiconductors [27] and aid in identifying the role of magnetic impurities in doped insulators showing ferromagnetic properties [28].

We acknowledge financial support from the Access to Major research Facilities Programme and Australian Research Council.

\*Thomas.Saerbeck@ansto.gov.au

- [1] D. D. Awschalom and M. E. Flatte, *Nature Phys.* **3**, 153 (2007).
- [2] G. J. Strijkers *et al.*, *Phys. Rev. Lett.* **84**, 1812 (2000).
- [3] T. Dietl, *Nature Mater.* **9**, 965 (2010).
- [4] J. M. D. Coey *et al.*, *Nature Mater.* **4**, 173 (2005).
- [5] D. A. Abanin and D. A. Pesin, *Phys. Rev. Lett.* **106**, 136802 (2011).
- [6] P. M. Koenraad and M. E. Flatte, *Nature Mater.* **10**, 91 (2011).
- [7] M. Schaefer *et al.*, *J. Appl. Phys.* **77**, 6432 (1995).
- [8] J. C. Slonczewski, *J. Appl. Phys.* **73**, 5957 (1993).
- [9] S. Bosu *et al.*, *Phys. Rev. B* **81**, 054426 (2010).
- [10] M. J. Wilson *et al.*, *Phys. Rev. B* **81**, 045319 (2010).
- [11] Y. Kobayashi *et al.*, *Phys. Rev. B* **59**, 3734 (1999).
- [12] H. Zabel *et al.*, in *Handbook of Magnetism and Advanced Magnetic Materials*, edited by H. Kronmüller and S. Parkin (John Wiley and Sons, New York, 2007), Vol. 3.
- [13] B. Toperverg (unpublished).
- [14] T. Saerbeck *et al.* (to be published).
- [15] S. O. Demokritov, *J. Phys. D* **31**, 925 (1998).
- [16] Measured by fluorescence detection at 25° incident angle using the TBT XMCD station on the SIM beam line, Swiss Light Source, Switzerland.
- [17] J. Dresselhaus *et al.*, *Phys. Rev. B* **56**, 5461 (1997).
- [18] E. Stavitski and F. M. F. de Groot, *Micron* **41**, 687 (2010).
- [19] N. Loh, Ph.D. thesis, University of Western Australia, 2011.
- [20] P. Bruno and C. Chappert, *Phys. Rev. B* **46**, 261 (1992).
- [21] J. C. Slonczewski, *Phys. Rev. Lett.* **67**, 3172 (1991).
- [22] S. Schwieger and W. Nolting, *Phys. Rev. B* **69**, 224413 (2004).
- [23] The form of the laterally varying loose spin coupling for the left ferromagnet A is

$$J_1^{\text{LSC,A}} = \frac{1}{2} \{ F[J_{\text{Co-Mn}}^{\text{RKKY}}(x, y, z) - U_B(z)M_{\text{Mn}}] - F[J_{\text{Co-Mn}}^{\text{RKKY}}(x, y, z) + U_B(z)M_{\text{Mn}}] \}.$$

The equation is symmetrically valid for ferromagnet B.

- [24] M. D. Stiles, in *Nanomagnetism: Ultrathin Films, Multilayers and Nanostructures*, edited by D. Mills and J. A. C. Bland (Elsevier, New York, 2006), Vol. 1.
- [25] B. Heinrich *et al.*, *J. Magn. Magn. Mater.* **140–144**, 545 (1995).
- [26] Y. Sakuraba *et al.*, *J. Phys. D* **44**, 064009 (2011).
- [27] J. H. Chung *et al.*, *Phys. Rev. Lett.* **101**, 237202 (2008).
- [28] J. J. I. Wong *et al.*, *Phys. Rev. B* **81**, 094406 (2010).